

MSEC2018-6562

LIGHTWEIGHT MICROLATTICE WITH TUNABLE MECHANICAL PROPERTIES USING 3D PRINTED SHAPE MEMORY POLYMER

Chen Yang

Department of Mechanical and
Aerospace Engineering,
Rutgers, The State University of New Jersey
Piscataway, NJ, United States

Andrew Dopp

Department of Mechanical and
Aerospace Engineering,
Rutgers, The State University of New Jersey
Piscataway, NJ, United States

Manish Boorugu

Department of Mechanical and
Aerospace Engineering,
Rutgers, The State University of New Jersey
Piscataway, NJ, United States

Howon Lee

Department of Mechanical and
Aerospace Engineering,
Rutgers, The State University of New Jersey
Piscataway, NJ, United States

ABSTRACT

Metamaterials are architected artificial materials engineered to exhibit properties not typically found in natural materials. Increasing attention has recently been given to mechanical metamaterials with unprecedented mechanical properties including high stiffness, strength, or/and resilience even at extremely low density. These unusual mechanical performances emerge from the three-dimensional (3D) spatial arrangement of the micro-structural elements designed to effectively distribute mechanical loads. Recent advances in additive manufacturing in micro-/nano- scale have catalyzed the growing interest in this field.

This work presents a new lightweight microlattice with tunable and recoverable mechanical properties using a three-dimensionally architected shape memory polymer (SMP). SMP microlattices were fabricated utilizing our micro additive manufacturing technique called projection micro-stereolithography (PμSL), which uses a digital micro-mirror device (DMD™) as a dynamically reconfigurable photomask. We use a photo-crosslinkable and temperature-responsive SMP which can retain its large deformation until heated for spontaneous shape recovery. In addition, it exhibits remarkable elastic modulus changes during this transition. We demonstrate that mechanical responses of the micro 3D printed SMP microlattice can be reversibly tuned by temperature control. Mechanical testing result showed that stiffness of a SMP microlattice changed by two orders of magnitude by a moderate temperature shift by 60°C. Furthermore, the shape memory effect of the SMP allows for full restitution of the original shape of the microlattice upon heating even after substantial

mechanical deformation. Mechanical metamaterials with lightweight, reversibly tunable properties, and shape recoverability can potentially lead to new smart structural systems that can effectively react and adapt to varying environments or unpredicted loads.

INTRODUCTION

A cellular solid is an assembly of small compartments (cells) with connected solid edges or faces. They have existed in nature for centuries and widely found in many species due to their exceptional mechanical properties at low weight [1]. These mechanical efficient materials including honeycombs [2] and foams, like sponges [3], and cancellous bone [4] inherit their unique properties from their fiber level topology in structural arrangement. For example, yew behaves much lower longitudinal stiffness in tensile test comparing to spruce due to its larger microfibril angle (15° – 20° for yew and 0° – 5° for spruce) [5], which makes yew a compliant softwood and spruce a hard building wood.

By mimicking the idea of using specific structural arrangement to fill the space, researchers have designed engineered lightweight material (lightweight microlattice) with unseen mechanical properties such as strength, stiffness and resilience. Due to the high structural complexity (slender micro struts, void spaces, and various angles between struts) and requirement of dimensional accuracy, it has been a formidable challenge to manufacture the lightweight microlattices using traditional manufacturing tool such as molding and machining. Numerous lightweight microlattices was realized recently as a result of evolution in micro additive manufacturing [6]–[14].

The mechanical properties of lightweight microlattices are determined from the properties of their constituent material, relative density and structural design. Depending on the form of connection between cells, there are two categories of foams defined: open-cell foams, in which cells connect through edges, and closed-cell foams, which are connected through planes. Open-cell foams includes stretching-dominated and bending-dominated microlattices. Much effort has been focused on printing microlattices with different structural design with determined governing relationship between stiffness and relative density. A commonly used scaling relation determining the proportional relation of relative stiffness (effective stiffness E /stiffness of constituent material E_0) and relative density (effective density ρ /stiffness of constituent material ρ_0) of microlattice is $\frac{E}{E_0} \sim \left(\frac{\rho}{\rho_0}\right)^n$, where the exponent n is 1 for stretching-dominated lattices and n is 2 for bending-dominated lattices [15]. Zheng *et al.* presented 3D printed Octet-Truss microlattice with $n = 1$ and tetradehedron microlattice (Kelvin foam) with $n = 2$ [10]. HRL (pyramidal) [8], [9] and Octahedron [13], [14] lattices are another engineering microlattices with $n = 2$. Hierarchical architectures have been reported combining bending-dominated and stretching-dominated structures at different length scale [11], [12]. Regardless of constituent materials used and the scaling laws between stiffness and density, mechanical properties of the microlattices are fixed and irreversible after the microstructural design is physically realized through manufacturing. Although it has been reported that tunable stiffness in microlattice was achieved by using wax coating on 3D printed polyurethane cubic lattice [16], its reversibility was limited because the coated wax melts away above 75°C resulting in a failure of the material.

In this work, we achieved reversibly tunable mechanical properties in lightweight microlattices by employing an additive micro-manufacturing technique and a tunable constituent material. By actively tuning the properties of a stimuli-responsive material, desired mechanical property of the microlattice can be achieved simply by controlling environmental conditions. Here we use a photo-crosslinkable and temperature-responsive shape memory polymer (SMP) as the constituent material. Not only does this SMP exhibit thermally triggered shape recovery from large deformation and shape fixing, it also shows a remarkable property transition between rigid and elastic states around its glass transition temperature (T_g). At temperature lower than the glass transition temperature, SMP is glassy and rigid. It deforms plastically and stay at the temporary shape. At temperature higher than the transition temperature, SMP is rubbery and soft. It deforms elastically and generates restoring force to recover to its original fabricated shape. This shape recovery behavior is called “shape memory effect” (SME) and has been widely used in many areas, especially in biomedical engineering for stent, micro-catheter, suture, and orthodontics [17]. It has been shown that a large span of material properties of SMPs, such as glass transition temperature, glassy and rubbery moduli, failure strain, and toughness can be achieved from different combinations of monomer and crosslinker [18], [19]. This variety in mechanical

properties of SMP allows the SMP microlattices to be tailored for a wide range of applications. In addition, SME permits full shape recovery of the microlattices to its original shape even after large deformation. Although several 3D printed structures using SMP have been reported demonstrating shape transformation from 2D to 3D or from one configuration to another in 3D space [20]–[25], utilizing mechanical property modulation to achieve tunable functions has not been reported.

We used projection micro-stereolithography (PμSL) to additively fabricate SMP microlattices in this work. PμSL is a rapid and high resolution photo-polymerization based additive manufacturing technique [26]–[28]. UV light from a light emitting diode (LED) is spatially modulated by a digital micro-mirror device (DMD™) which displays a computer-controlled pattern generated from a 3D CAD model. UV light reflected off the DMD™ passes through a projection lens and is focused on the surface of photo-curable resin. Resin in the illuminated area solidifies and form a layer of the projected pattern. After completing the layer, the sample holder drops down to fabricate the next layer. By repeating the cycles iteratively, PμSL creates a solid micro object layer-by-layer. In this manner, a PμSL system can rapidly manufacture complex 3D micro-structures at a microscale resolution.

In this paper, we present SMP microlattice structures printed by PμSL. The printed structures possess properties of lightweight, reversibly tunable modulus, and shape recoverability. We used tetradehedron microlattice (Kelvin foam microlattice), which is a bending-dominated open-cell foam, as the example. We printed four different samples with various relative densities to demonstrate the scaling law between mechanical stiffness and relative density. Compression testing at five different temperatures and measured effective stiffness showed tunability of more than two orders of magnitude. Shape fixing at low temperature and shape recovery at high temperature of SMP microlattice were also successfully demonstrated. As a potential thermally tunable smart structural material, desired mechanical properties can be achieved by simply adjusting temperature, which makes material suitable for various purposes. In addition, recoverability after large deformation ensures economic efficiency and environmental friendliness.

EXPERIMENTAL DESIGN

DESIGN OF MICROLATTICES

Bending-dominated and stretching-dominated architectures are two main categories of open-cell engineering microlattice. The stiffness of each architecture follows unique scaling laws regarding the relative density [29]. In this work, we chose Kelvin foam microlattice as the object of study. It is a bending-dominated structure, in which all struts exhibit bending behavior during load bearing. The relative density ρ/ρ_0 as a function of strut length l and diameter d and scaling relation between relative stiffness E/E_0 and relative density ρ/ρ_0 for Kelvin foam is shown in Equation 1 and 2 [30].

$$\rho/\rho_0 = 3\pi d^2/8\sqrt{2}l^2 \quad (1)$$

$$E/E_0 = 1.007 \cdot (\rho/\rho_0)^2 \quad (2)$$

RESIN PREPARATION

All chemicals including the monomer, crosslinker, photo initiator (PI), and photo absorber (PA) were purchased from Sigma-Aldrich (St. Louis, MO, USA) and used as received. Tert-Butyl Acrylate (monomer) at the concentration of 80% by weight and Poly(ethylene glycol) diacrylate Mn 250 (crosslinker) at the concentration of 20% by weight were mixed together in an amber bottle. 2% by weight of Phenylbis(2,4,6-trimethylbenzoyl) phosphine (PI) and 0.1% by weight of Sudan I (PA) were then added into the polymer resin.

CHARACTERIZATION OF THERMOMECHANICAL PROPERTIES OF SMP

To prepare sample for thermomechanical properties, resin was added into a glass mold with 1 mm gap and cured using a UV oven (365 nm) for 20 min on each side. Then the obtained 1 mm thick film was laser cut into 40 mm x 10 mm x 1 mm rectangular sample. Thermomechanical properties such as storage and loss moduli and glass transition temperature of shape memory polymer were measured using TA Q800 Dynamic Mechanical Analysis (DMA) machine with temperature ramp of 1 °C/min from 30°C to 90°C, frequency 1 Hz, strain amplitude 0.2%, preload 0.001N and force track 150%.

PμSL PROCESS

A custom-made PμSL system was built in this work. It consists of a UV LED (365 nm), a digital micro-mirror device (DMD), a linear stage, and a projection lens. The power adjustable UV LED (Hamamatsu, L10561) shines on a high resolution DMD™ (Texas Instruments, DLPLCR6500EVM). Then patterned UV light is projected through a projection lens (Thorlabs) and to focus the light on the top surface of resin. Once a layer is formed, the linear stage (Thorlabs, MTS50-Z8) moves down by designed layer thickness after each projection. Parameters in printing process include light intensity, layer thickness, and curing time. We used light intensity of 29 mW/cm², layer thickness of 100 μm, curing time of 50 sec. Whole system was in a UV blocking enclosure. The oxygen concentration was maintained at 1% by pumping nitrogen gas.

POST-PROCESSING

Samples after printing were rinsed in ethanol for 1 min to remove uncured resin. Postcuring of printed structure was done by thermal processing: 2 g of ammonium persulfate (Sigma-Aldrich, St. Louis, MO, USA) were dissolved in 100 g of DI water as the thermal curing agent. Printed sample was soaked in the solution and heated in a temperature oven at 90°C for 12 h to ensure full crosslinking.

RELATIVE DENSITY MEASUREMENT

Effective density ρ of printed sample was measured using mass divided by total volume of the lattice. Bulk density ρ_0 of SMP was obtained from a printed solid cylinder using the same method.

COMPRESSION TEST

To obtain stiffness of printed structure at different temperature, compression test was conducted using the setup shown in Figure 1. Peltier heater (Technology, inc. CP-061HT) heats up the air chamber where sample sit. A 50 N load cell (Omega, LCMFL-50N) attached to a motorized stage (Thorlabs, LTS150) moved down at 0.1% strain per sec to compress the sample. Thermocouple mounted in the chamber monitored the temperature inside. Force from load cell and temperature from thermocouple were recorded using NI DAQ and LabVIEW. Force and displacement information obtained from LabVIEW were converted to stress and strain curve, which was used to extract the stiffness of printed structure. One sample was tested three times, and the average stiffness, maximum and minimum stiffness were obtained.

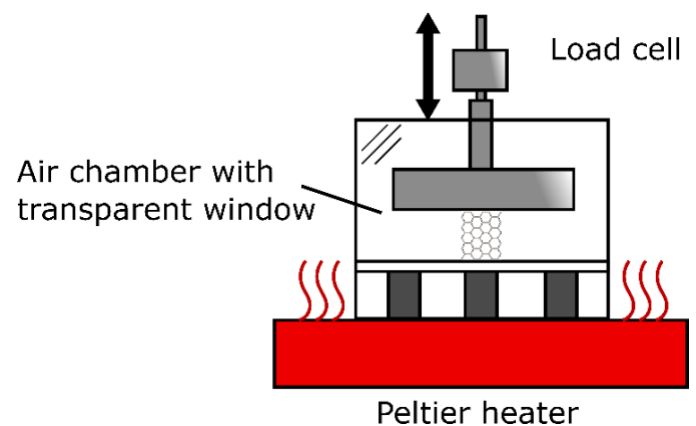


Figure 1. Schematic drawing of setup for temperature dependent stiffness

SHAPE MEMORY EFFECT

Using the same setup in compression test, SME of 3D printed microlattice was demonstrated: First, the air chamber was heated to 70°C and stage moved down to compress the sample. Second, Peltier in cooling mode brought the temperature inside the chamber down to 20°C to fix the temporary shape. Third, top plate was removed to show fixity of sample at low temperature. Last, Peltier heated the air chamber again to recover to its permanent shape.

RESULTS AND DISCUSSION

Storage modulus, loss modulus and tan delta as a function of temperature were tested using DMA with parameters listed earlier. Figure 2 shows results for tBA:PEGDA250 8:2 PI 2% SMP film. The storage modulus changes by more than two orders of magnitude from 30°C to 90°C. Loss modulus that indicates the viscous dissipation inside the polymer also changes and reaches its maximum around 50°C. Tan Delta value shows a peak at 63°C that is the glass transition temperature of this SMP.

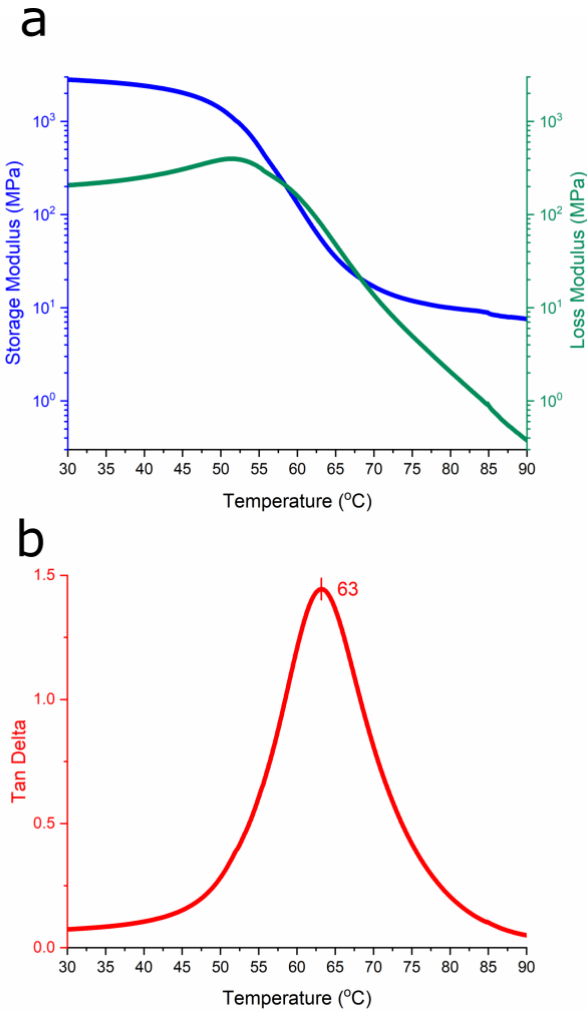


Figure 2. (a) Storages modulus and Loss modulus vs. temperature, (b) Tan Delta of tBA:PEGDA250 8:2

We printed four Kelvin foam microlattices with different relative densities as shown in Figure 3. Their designed strut length l , diameter d , relative density, and measured mass m , volume V , relative densities are all listed in Table 1. Each sample has dimension of approximately 10 mm x 10 mm x 9 mm. In Figure 3, from left to right, samples are numbered as KF 1 to 4.

3D Printed Kelvin foam microlattices using SMP as shown in Figure 3 has temperature dependent stiffness that comes from its constituent SMP. Figure 4a is the stress and strain curve of a 9.7% relative density Kelvin foam at 30°C, 45°C, 60°C, 75°C, and 90°C and Figure 4b is the corresponding stiffness. Stiffness value was extracted from the linear portion of stress and strain curve. It is clear that at low temperature, the SMP Kelvin foam microlattice's stiffness reaches 5.6MPa. While at high temperature, its stiffness is only 0.14MPa. The stiffness of the printed structure also changes by more than two orders of magnitude by a moderate temperature change of 60°C.

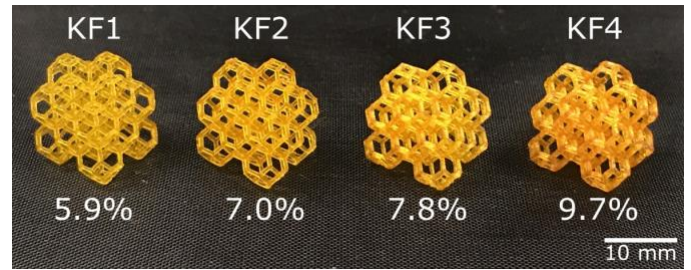


Figure 3. 3D printed Kelvin foam microlattices using SMP with 4 different relative densities

Table 1. Geometrical properties of printed Kelvin foam microlattices

Sample	l (um)	d (um)	Designed Relative Density	m (g)	V (mm ³)	Measured Relative Density
KF1	1380	338	5%	0.060	966.7	5.9%
KF2	1380	370	6%	0.071	956.3	7.0%
KF3	1380	400	7%	0.080	978.0	7.8%
KF4	1380	427	8%	0.104	1022.9	9.7%

In spite of the effect from temperature change, mechanical stiffness of Kelvin foam microlattices still follows the scaling law related to relative density. In Figure 5, stiffness of Kelvin foam microlattices with four different relative densities are plotted. At each temperature, a linear relationship can be drawn from the curve that indicates the stiffness of this bending-dominated structure is determined by structural design and its relative density. The slopes that similar to 2 on this log-log plot matches with the scaling law $\frac{E}{E_s} \sim \frac{\rho^2}{\rho_s}$. This scaling law is preserved at all temperature. For all microlattices, there is more than two orders of magnitude difference in stiffness when temperature changes from 30°C to 90°C.

3D printed Kelvin foam microlattice inherits shape memory capability from its constituent shape memory polymer. To demonstrate its shape memory effect, the initial state of this microlattice was shown in Figure 6a. When compressed at 70°C by 8% as in Figure 6b and then cooled down to 20°C, SMP Kelvin foam fixed the deformed temporary shape as in Figure 6c. In glassy state, SMP Kelvin foam was able to hold its shape until it was heated again. Upon heating, the microlattice recovered to its original shape as in Figure 6d. Red dotted line in Figure 6 indicates the permanent height of sample and blue dotted line marks the temporary height during compression. This SME experiment of Kelvin foam microlattice also demonstrates recoverability of structure upon heating. The strain of compression was limited by the stretchability at high temperature. Strain beyond 9% resulted in fracture in structure. With a more stretchable SMP, a more significant recoverability will be shown.

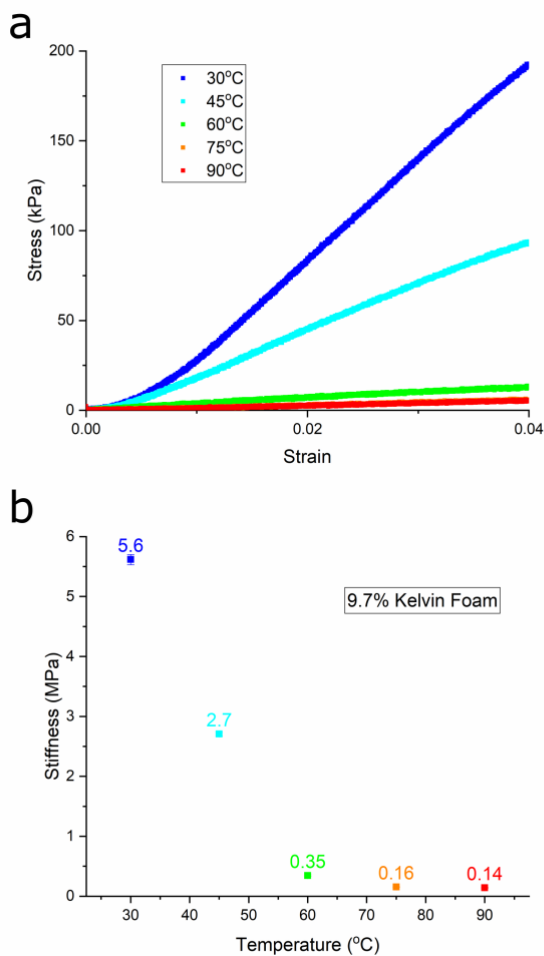


Figure 4. (a) Stress vs strain curve of 9.7% SMP Kelvin foam at 5 temperatures, (b) Stiffness of 9.7% SMP Kelvin foam at 5 temperatures

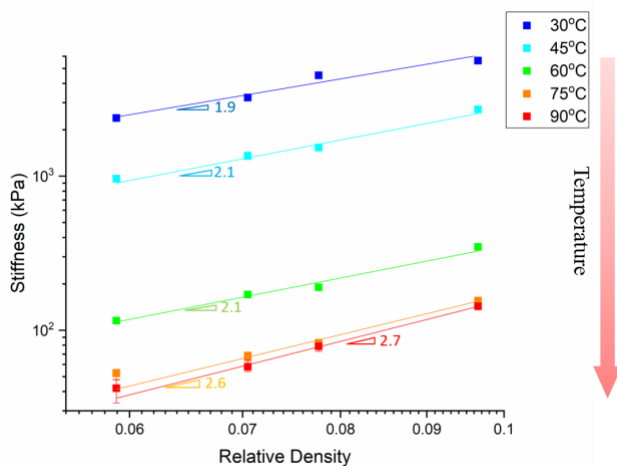


Figure 5. Stiffness of 4 Kelvin foam samples with different relative densities at 5 different temperatures

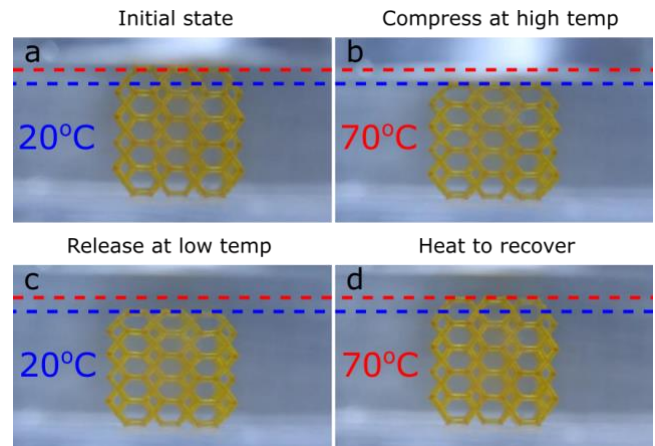


Figure 6. SME of SMP Kelvin foam: (a) Initial state, (b) Compress sample by 8% at 70°C, (c) Release the top plate at 20°C, (d) Sample recovers upon heating

CONCLUSION

In this work, we demonstrated 3D printed Kelvin foam microlattices using SMP. TBA 80% + PEGDA 20% was used as the constituent SMP. It has a glass transition temperature of 63 °C and its elastic modulus changes by more than two orders of magnitude from 2.9 GPa at 30 °C to 7.8 MPa at 90 °C. Unlike widely reported microlattices whose stiffness is fixed once manufactured, our microlattices inherit the thermally responsive stiffness from the constituent SMP. They show a stiffness change by more two orders of magnitude with a temperature span of 60°C. For a Kelvin foam with a relative density of 9.7 %, its stiffness of 5.6 MPa at 30 °C decreases to 0.14 MPa at 90 °C. From all four samples having different relative densities, we observed that stiffness still depended on its structural design at each temperature and the scaling law with the exponent of 2 for bending-dominated lattices was preserved. Furthermore, shape fixing at low temperature and shape recovery at high temperature were successfully demonstrated from 3D printed SMP microlattices. The mechanical metamaterials with lightweight, tunable properties and recoverability can potentially lead to new smart structural systems that can effectively react and adapt to varying environments or unpredicted loads.

ACKNOWLEDGEMENTS

This work was supported by Rutgers School of Engineering Startup Fund, Rutgers University Research Council Grant, and Defense Acquisition Program Administration and Agency for Defense Development under the contract UD150032GD.

REFERENCES

- [1] P. Fratzl and R. Weinkamer, "Nature's hierarchical materials," *Prog. Mater. Sci.*, vol. 52, no. 8, pp. 1263–1334, Nov. 2007.
- [2] K. Ando and H. Onda, "Mechanism for deformation of wood as a honeycomb structure II: First buckling mechanism of cell walls under radial compression using the generalized cell model," *J. Wood Sci.*, vol. 45, no. 3, pp. 250–253, Jun. 1999.

- [3] J. Shen, Y. M. Xie, X. Huang, S. Zhou, and D. Ruan, "Behaviour of luffa sponge material under dynamic loading," *Int. J. Impact Eng.*, vol. 57, no. Supplement C, pp. 17–26, Jul. 2013.
- [4] "Bones," *Princeton University Press*. [Online]. Available: <https://press.princeton.edu/titles/7313.html>. [Accessed: 08-Nov-2017].
- [5] D. Keunecke, M. Eder, I. Burgert, and P. Niemz, "Micromechanical properties of common yew (*Taxus baccata*) and Norway spruce (*Picea abies*) transition wood fibers subjected to longitudinal tension," *J. Wood Sci.*, vol. 54, no. 5, p. 420, Oct. 2008.
- [6] J. Bauer, L. R. Meza, T. A. Schaedler, R. Schwaiger, X. Zheng, and L. Valdevit, "Nanolattices: An Emerging Class of Mechanical Metamaterials," *Adv. Mater.*, vol. 29, no. 40, p. n/a–n/a, Oct. 2017.
- [7] N. A. Fleck, V. S. Deshpande, and M. F. Ashby, "Micro-architected materials: past, present and future," *Proc. R. Soc. Math. Phys. Eng. Sci.*, vol. 466, no. 2121, pp. 2495–2516, Sep. 2010.
- [8] A. J. Jacobsen, W. Barvosa-Carter, and S. Nutt, "Compression behavior of micro-scale truss structures formed from self-propagating polymer waveguides," *Acta Mater.*, vol. 55, no. 20, pp. 6724–6733, Dec. 2007.
- [9] T. A. Schaedler *et al.*, "Ultralight Metallic Microlattices," *Science*, vol. 334, no. 6058, pp. 962–965, Nov. 2011.
- [10] X. Zheng *et al.*, "Ultralight, ultrastiff mechanical metamaterials," *Science*, vol. 344, no. 6190, pp. 1373–1377, Jun. 2014.
- [11] L. R. Meza, A. J. Zelhofer, N. Clarke, A. J. Mateos, D. M. Kochmann, and J. R. Greer, "Resilient 3D hierarchical architected metamaterials," *Proc. Natl. Acad. Sci.*, vol. 112, no. 37, pp. 11502–11507, Sep. 2015.
- [12] X. Zheng *et al.*, "Multiscale metallic metamaterials," *Nat. Mater.*, vol. 15, no. 10, p. nmat4694, Jul. 2016.
- [13] L. R. Meza and J. R. Greer, "Mechanical characterization of hollow ceramic nanolattices," *J. Mater. Sci.*, vol. 49, no. 6, pp. 2496–2508, Mar. 2014.
- [14] D. Jang, L. R. Meza, F. Greer, and J. R. Greer, "Fabrication and deformation of three-dimensional hollow ceramic nanostructures," *Nat. Mater.*, vol. 12, no. 10, pp. 893–898, Sep. 2013.
- [15] "Cellular Solids," *Cambridge University Press*. [Online]. Available: <http://www.cambridge.org/se/academic/subjects/engineering/materials-science/cellular-solids-structure-and-properties-2nd-edition?format=PB>. [Accessed: 25-Jan-2016].
- [16] N. G. Cheng, A. Gopinath, L. Wang, K. Iagnemma, and A. E. Hosoi, "Thermally Tunable, Self-Healing Composites for Soft Robotic Applications: Thermally Tunable, Self-Healing Composites ...," *Macromol. Mater. Eng.*, vol. 299, no. 11, pp. 1279–1284, Nov. 2014.
- [17] W. Small, IV, P. Singhal, T. S. Wilson, and D. J. Maitland, "Biomedical applications of thermally activated shape memory polymers," *J. Mater. Chem.*, vol. 20, no. 17, p. 3356, 2010.
- [18] D. L. Safranski and K. Gall, "Effect of chemical structure and crosslinking density on the thermo-mechanical properties and toughness of (meth)acrylate shape memory polymer networks," *Polymer*, vol. 49, no. 20, pp. 4446–4455, Sep. 2008.
- [19] C. M. Yakacki, R. Shandas, D. Safranski, A. M. Ortega, K. Sassaman, and K. Gall, "Strong, Tailored, Biocompatible Shape-Memory Polymer Networks," *Adv. Funct. Mater.*, vol. 18, no. 16, pp. 2428–2435, Aug. 2008.
- [20] Q. Ge, H. J. Qi, and M. L. Dunn, "Active materials by four-dimension printing," *Appl. Phys. Lett.*, vol. 103, no. 13, p. 131901, 2013.
- [21] Q. Ge, C. K. Dunn, H. J. Qi, and M. L. Dunn, "Active origami by 4D printing," *Smart Mater. Struct.*, vol. 23, no. 9, p. 094007, Sep. 2014.
- [22] K. Yu, A. Ritchie, Y. Mao, M. L. Dunn, and H. J. Qi, "Controlled Sequential Shape Changing Components by 3D Printing of Shape Memory Polymer Multimaterials," *Procedia IUTAM*, vol. 12, pp. 193–203, 2015.
- [23] Y. Mao, K. Yu, M. S. Isakov, J. Wu, M. L. Dunn, and H. Jerry Qi, "Sequential Self-Folding Structures by 3D Printed Digital Shape Memory Polymers," *Sci. Rep.*, vol. 5, p. 13616, Sep. 2015.
- [24] Q. Ge, A. H. Sakhaei, H. Lee, C. K. Dunn, N. X. Fang, and M. L. Dunn, "Multimaterial 4D Printing with Tailorable Shape Memory Polymers," *Sci. Rep.*, vol. 6, p. srep31110, Aug. 2016.
- [25] M. Zarek, M. Layani, I. Cooperstein, E. Sachyani, D. Cohn, and S. Magdassi, "3D Printing of Shape Memory Polymers for Flexible Electronic Devices," *Adv. Mater.*, p. n/a–n/a, Sep. 2015.
- [26] C. Sun, N. Fang, D. M. Wu, and X. Zhang, "Projection micro-stereolithography using digital micro-mirror dynamic mask," *Sens. Actuators Phys.*, vol. 121, no. 1, pp. 113–120, May 2005.
- [27] X. Zheng *et al.*, "Design and optimization of a light-emitting diode projection micro-stereolithography three-dimensional manufacturing system," *Rev. Sci. Instrum.*, vol. 83, no. 12, p. 125001, 2012.
- [28] Y. M. Ha, J. W. Choi, and S. H. Lee, "Mass production of 3-D microstructures using projection microstereolithography," *J. Mech. Sci. Technol.*, vol. 22, no. 3, p. 514, Mar. 2008.
- [29] V. S. Deshpande, M. F. Ashby, and N. A. Fleck, "Foam topology: bending versus stretching dominated architectures," *Acta Mater.*, vol. 49, no. 6, pp. 1035–1040, Apr. 2001.
- [30] H. X. Zhu, J. F. Knott, and N. J. Mills, "Analysis of the elastic properties of open-cell foams with tetrakaidecahedral cells," *J. Mech. Phys. Solids*, vol. 45, no. 3, pp. 319–343, Mar. 1997.